REVIEW

Shape oscillating bubbles: hydrodynamics and mass transfer - a review

M. Martín[1], M. A. Galán[1], R. L. Cerro[2] and F. J. Montes*[1]

The subject of bubble oscillations, the associated hydrodynamics and the effect of bubbles on mass transfer in gas–liquid contact equipment, is reviewed. The emphasis is on rising and shape oscillating bubbles (n>0 mode) with little or negligible apparent volume change, rather than on volume oscillations (n=0 mode). Bubbles, as they move in liquid media, are subjected to forces that try to deform them as well as forces that try to keep them as individual entities, resulting in the fact that bubble contact area changes in time and so do the velocity profiles surrounding them. As a result, the concentration profiles are also affected, influencing the Sherwood number and the mass transfer rates from the gas phase to the liquid phase. The physical properties of the phases as well as bubble coalescence and breakup processes that occur within the equipment play an important role in defining the oscillation amplitude and decay. Thus, we summarise the main results and the theories behind bubble dynamics and mass transfer of oscillating bubbles, in search of further understanding of a phenomenon that has been under study for the past 50 years, yet is still far from being well understood or widely applied in the design of gas–liquid contact equipment.

Keywords: Gas–liquid mass transfer, Oscillating bubbles, Sherwood number, Coalescence, Review

Introduction

The origin of the study of bubble oscillations is based on the search for physical understanding of different phenomena, such as jet stability and cavitation in ship propellers and pumps,[1–14] underwater explosions,[15] gas–liquid contact for mass transfer purposes[16–20] and even in the recent claim of cold fusion in sonoluminiscence.[21,22] In this review, we focus on the study of oscillating bubbles in gas–liquid contact equipment because of the high impact that they have on the chemical industry, where it is considered that 25% of all chemical reactions take place in multiphase gas–liquid flow. A few significant examples are processes, such as waste water treatment, aerobic fermentations, CO_2 capture or algae growing where there is a large potential for efficiency improvement if we gain a deeper understanding of this particular phenomenon.[23]

Mass transfer is often the limiting variable and the design parameter of the above mentioned processes. Thus, an accurate prediction of the volumetric mass transfer coefficient is required for the proper design of such equipment where bubbles are often not rigid but oscillating.[24] Bubble oscillations do determine not only the bubble shape and contact area, but also the hydrodynamics surrounding the bubbles, the rising velocity (and hold-up), as well as the concentration profiles which define the mass transfer from the gas phase to the liquid phase. Several authors have found that oscillations have a favourable effect on gas transfer to the liquid phase[16,25–27] by reducing the bubble rising velocity and increasing the gas hold up.[16,28–30] However, so far, most of the design equations are empirical correlations based on dimensionless numbers and adjustable parameters, thus affected by the geometry of the system, the range of the operating variables and even the experimental methods used in the determination of the mass transfer coefficients.[17,18,23,31–33] In order to have a deeper understanding of the large number of variables defining the mass transfer rate and, in particular, the effect of bubble oscillation, theoretical models are useful. Even though the idea of bubble oscillations can be traced back into the literature to the beginning of the last century due to Lord Rayleight,[3] its evaluation and implementation for predicting the mass transfer rates has been postponed, and it has not been till very recently that the effect of the oscillation of the bubbles either as responsible for bubble shape[18] or to define the Sherwood number (Sh=$k_L/d_b/D_{AB}$, where k_L is the liquid film resistance, d_b the bubble diameter and D_{AB} the diffusion coefficient) and the contact area a, has been used to predict mass transfer in bubble columns.[19,20,32,33]

This review is organised as follows. We first describe the hydrodynamic principles of bubble oscillation to characterise this particular motion and the variables that describe it, frequency, amplitude and decay, as well as

[1]Departamento de Ingeniería Química. Universidad de Salamanca, Pza. de los Caídos 1-5, Salamanca 37008, Spain
[2]Department of Chemical and Materials Engineering, University of Alabama in Huntsville, Huntsville, AL 35899, USA

*Corresponding author, email javimon@usal.es

Received 2 August 2011; accepted 1 November 2011
DOI 10.1179/1758897911Y.0000000006

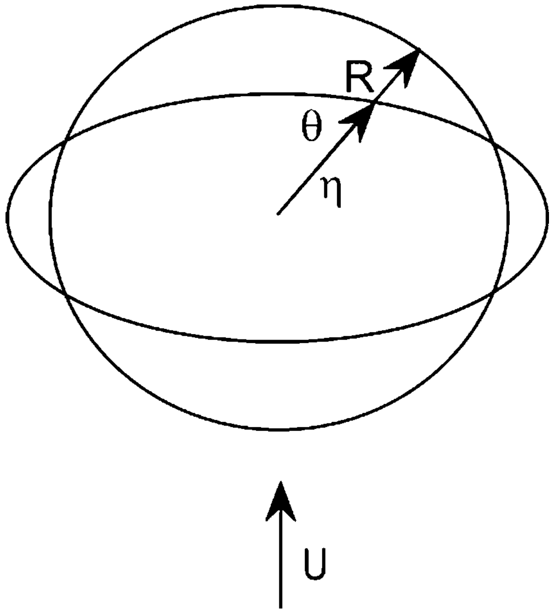

1 Scheme of bubble oscillations

the different approaches to model it. In the section on 'Effect of bubble deformation and oscillation on mass transfer', we study the effect of bubble oscillations on the mass transfer rates and the modelling efforts (either analytical approximations or numerical solutions) to compute the Sherwood number of the bubbles. In the section on 'Bubble coalescence: contact area versus bubble oscillation', we evaluate the trade-off that coalescence presents on the mass transfer: contact area versus mass transfer enhancement due to the oscillations. Finally, in the section on 'Mass transfer in bubble columns', we describe the modelling of bubble columns capturing the effect of bubble oscillations on the Sherwood number and on the gas–liquid contact area. It should be noted that the emphasis of the review is on rising and shape oscillating bubbles ($n>0$ mode) with little or negligible apparent volume change, rather than on volume oscillations ($n=0$ mode).

Hydrodynamics of bubble oscillations

In this section, we first discuss the phenomenon from the physical stand point trying to gain background and to identify the variables that characterise it. Next, we comment on the theoretical basis proposed in the literature to understand and model bubble oscillations.

Bubbles not affected by external forces assume a static shape which, in the case of small bubbles, is close to a sphere, since the interfacial tension effect dominates the gravitational effect. If such a bubble gets deformed by an external non-continuous force, the bubble will return to its initial shape after a certain period of time. Assuming the bubble is spherically symmetric at the start, we can distinguish mainly two stages during the bubble oscillation process (see Fig. 1). First, the expansion phase, where the bubble still remains more or less spherical, next the collapse phase when oscillation and surface wave motion take place. Bubble oscillations are also usually described as the result of wake shedding, with the onset of oscillations coinciding with the onset of vortex shedding from the wake.[34,35]

In Figs. 2 and 3, we present photographs of the onset of the oscillations after different hydrodynamic processes common in gas–liquid contact equipment. For instance, Fig. 2 shows the photographs of the oscillations induced after bubble detachment from a sieve plate. The orifice diameter D_o is 2 mm and the gas flow rate Q_c used is 5×10^{-6} m^3 s^{-1} for all cases, but the liquid media is modified by the addition of carboxymethyl cellulose to water. It can be seen that the process usually involves a series of oscillations whose amplitude decreases. Furthermore, as the liquid viscosity increases (with the increment in the concentration of carboxymethyl cellulose), bubble oscillations are attenuated and the shape of the bubbles is smoother, since the surface waves decay at an earlier stage. Therefore, the physical properties also play an important role in determining the decay of the oscillations.

Bubble detachment is not the most important process for the onset of bubble oscillations in contact equipment, but bubble interacts with other bubbles, such as bubble collisions, coalescence and break.[19,20,32,33] Figure 3 shows examples of these processes. Figure 3*a* and *b* represents the collision of two bubbles generated from two equal orifices of 2 mm separated from center to centre (Sep) 4 and 6·5 mm respectively. Figure 3*a* shows that the two bubbles collide resulting in bubble deformation and surface waves, but they do not coalesce while if the separation between the orifices is smaller, Sep=4 mm as seen in Fig. 3*b*, the contact time increases and the collision results in coalescence, generating in a bigger and more deformable bubble with smaller contact area than the two original bubbles. Finally, Fig. 3*c* represents bubble breakup under stirring. Breakup occurs after bubble deformation until the critical point is reached.[36] Then, the bubble breaks down into two daughter bubbles which oscillate until a shape in accordance with their size is reached. The sequence of collisions and breakup processes as a result of the fluid flow are responsible for maintaining the bubble oscillations over time.[20]

As it can be seen in the photographs presented in Figs. 2 and 3, the phenomenon of bubble oscillation is the result of a complex dynamic process involving viscous, surface tension, inertial and external forces. The intrinsic nature of the phenomenon has made use of the analogy with any other periodic phenomenon for its study and characterisation. Thus, the analysis of the oscillating phenomenon relies on energy and momentum balances to characterise the bubble oscillation features such as its amplitude, frequency and decay. If we now describe this problem from the first principles of fluid mechanics, at time 0, the initial stages correspond to irrotational flow and the energy dissipation comes from the surface pressure. As the time advances the vorticity generated at the free surface affects the liquid surrounding the bubble. For low viscosity fluids, the vorticity is negligible and the velocity field can be approximated by the inviscid flow where the irrotational approximation holds true. Otherwise, the dissipation of energy depends on the distribution of vorticity and the irrotational approximation is not valid.[38–45]

With this overview in mind, we are going to follow the literature available to present the approaches to model the oscillatory phenomenon of bubbles. The first studies on free oscillations date back to 1833 when Savart[1]

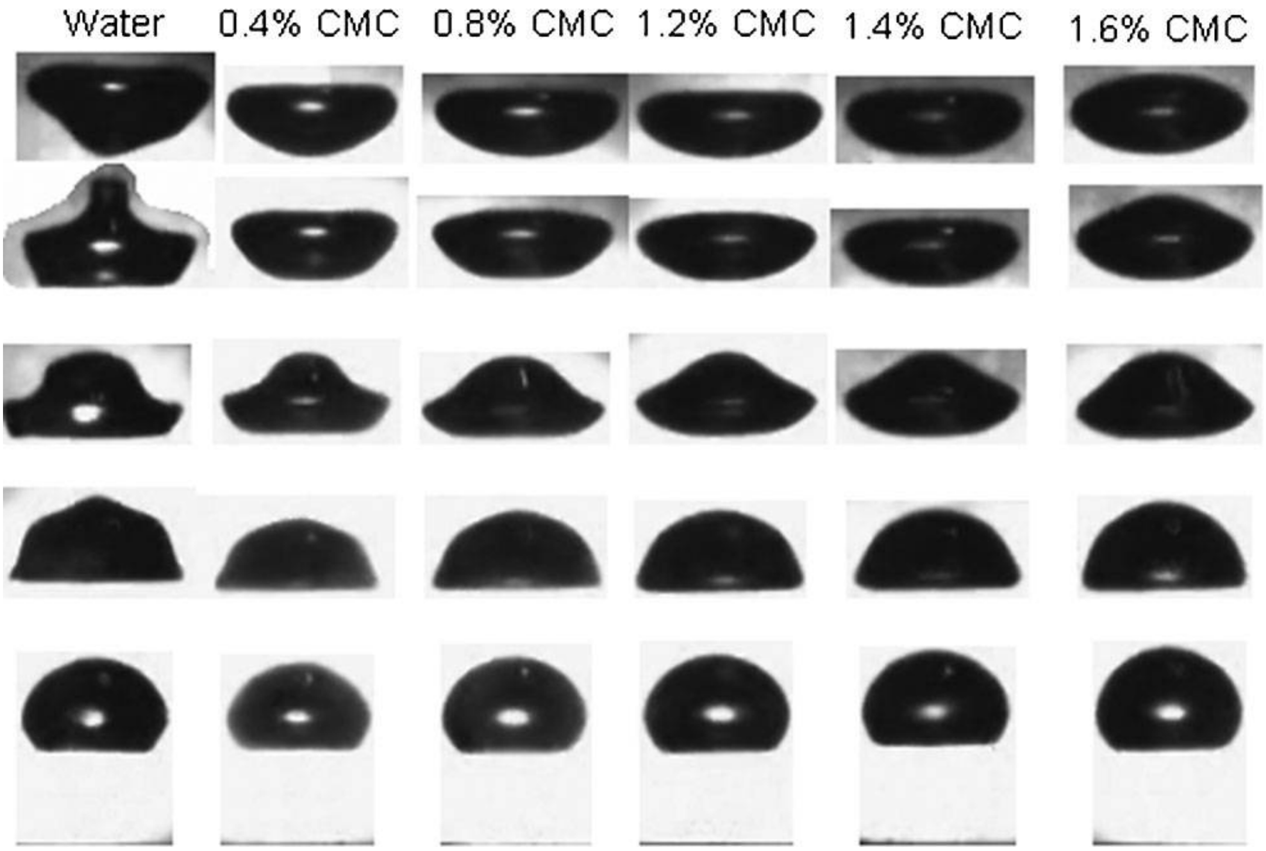

2 Effect of liquid viscosity on bubble oscillation: viscous decayment of bubbles oscillations D_o=2 mm; Q_c=5×10^{-6} m^3 s^{-1} (Ref. 37)

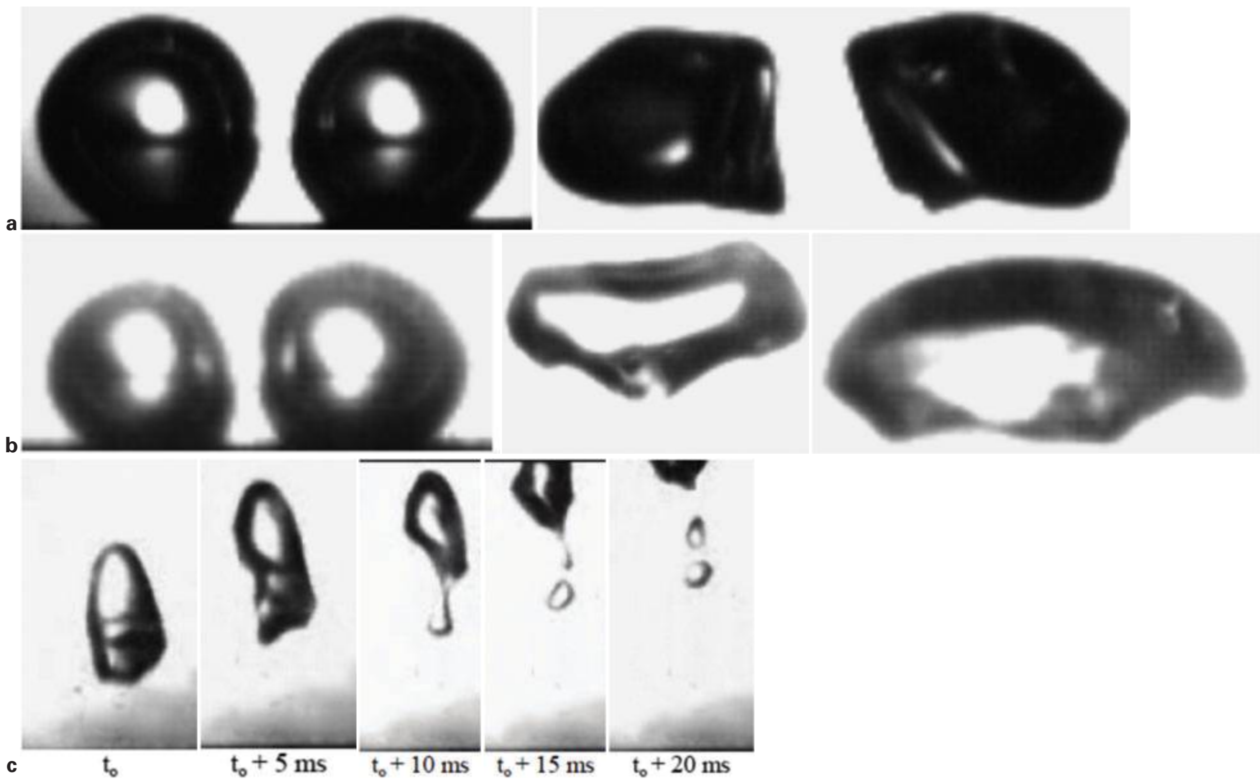

a bubble deformation after collision D_o=2·5 mm, Sep=6·5 mm, Q_c=0·6×10^{-6} m^3 s^{-1} (Refs. 111 and 134); *b* bubble deformation after coalescence D_o=2 mm, Sep=4 mm, Q_c=1·4×10^{-6} m^3 s^{-1} (Refs. 111 and 134); *c* bubble deformation after breakup; Rushton turbine H=5 cm, N=430 rev min^{-1}, Q_c=0·6×10^{-6} m^3 s^{-1} (Ref. 36)

3 Bubble oscillation after collision, coalescence and breakup

analysed the pulsation potions of the breakup of a liquid jet. The first theoretical contribution to that problem was delayed around 60 years.[2] In spite of these previous studies, the first contribution to the theoretical study of small amplitude oscillation of a particle whose stability was given by the surface tension was reported by Rayleigh in 1879[3] based on Plateau's work. Lord Rayleigh used dimensional analysis to determine the frequency of shape oscillations and he was also capable of identifying the modes of motion of bubbles using Legendre polynomials to calculate the oscillation frequencies using a linear approach. The analysis of Rayleigh is based on potential flow of an inviscid liquid neglecting the effect of the outside fluid. That paper reports a decrease in frequency with the increase in the amplitude of the oscillation which could not be explained at that point. It was Lamb[4] who in 1932 developed a model for the oscillation frequency when both fluids are inviscid. He solved the linearised Navier–Stokes (NS) equations based on a 'normal mode' approach. It was assumed that the effect of viscosity is small compared to the surface tension, which holds if a number of oscillations occur during the decay time. He also assumed that the oscillation amplitude is small compared to the bubble diameter and considered that the flow is irrotational, which is valid for fluids such as water. Under these conditions, the NS equation is simplified to the Laplace equation that is solved to calculate the frequency of oscillation given by equation (1)

$$\varpi_n = \left\{ (n-1)(n+1)(n+2)\frac{\sigma}{[(n+1)\rho_i + n\rho]R^3} \right\}^{1/2} \quad (1)$$

where n is the mode of oscillation, R the radius of the bubble, ρ the liquid density, ρ_i the gas density and σ the surface tension.

Even considering these assumptions, the model can provide an approximation of the frequency under many common operating conditions.[4,38,46] However, the approximation does not give rise to a viscous correction of the frequency.

With regard to the oscillation amplitude, A, the definition based on experimental measurements presented by Schroeder and Kintner,[40] given by equation (2) holds

$$A = \frac{d_{\max} - d_{\min}}{2d_{eq}} \quad (2)$$

where $d_{\max}$ and $d_{\min}$ are the maximum and minimum diameter of the bubble, while d_{eq} corresponds to the diameter of a spherical bubble with the same volume as the one under study.

Figure 2 shows an example of the effect of the dissipation of energy on bubble oscillation. Even though Lamb[4] derived models for predicting the oscillation decay, they were based on the assumption that only one phase was viscous and dense. It was Valentine *et al.*[38] who generalised the analysis and developed a simple model for evaluating the amplitude decay when both phases are viscous and dense. They solved an energy balance accounting for the phase inside and outside of the particle. The solution of the energy balance makes use of surface harmonics to write the velocity potentials for each of the phases and the kinetic energy. For an incompressible system the first law of thermodynamics yields

$$\frac{d\varepsilon_o}{dt} + \overline{F} = 0 \quad (3)$$

where the total energy of oscillation ε_o, involving the kinetic and potential energies (K and V respectively) of the external and internal phases (subscripts e and i) is given by equation (4)

$$\varepsilon_o = K_i + V_i + K_e + V_e =$$

$$\frac{R^3}{2}\sum_{n=2}^{\infty} A_n^2 \sigma_n^2 \left(\frac{\rho_i}{n} + \frac{\rho_e}{n+1}\right) \int_0^{2\pi}\int_0^{\pi} S_n^2(\theta,\phi)\sin\theta d\theta d\phi \quad (4)$$

And the energy of dissipation F is given by equation (5)

$$F_i = \mu_i R^2 \left\{ \frac{\partial}{\partial r}\frac{2}{\rho_i r^2}\frac{\partial K_i}{\partial r} \right\}_{r=R} \quad (5)$$

where R is the bubble radius, r, θ and ϕ the radial and angular coordinates in a spherical system, σ the surface tension, ρ the liquid density, n the mode of oscillation and S the surface harmonics. The dissipation energy F_i needs to be averaged over one cycle to determine $\overline{F}$ for equation (3). The solution to the equation allows including the effect of viscosity in the oscillation amplitude as presented in equation (6) as long as the viscosity is low[38,46]

$$A = A_o \exp[-t/\tau_n] \quad (6)$$

where A_o is the initial oscillation amplitude, t is time and τ_n is the time decay constant which turns out to be

$$\tau_n = \frac{R^2}{(n^2-1)v_i + n(n+2)v} \quad (7)$$

where R is the bubble radius, n the mode of oscillation and v is the specific viscosity of the phases where the subscript i refer to the phase within the particle. The dominant mode of oscillation is given by $n=2$, since $n=0$ and 1 correspond to bubble compression and displacement, whose terms have a small contribution in the energy balance.[38] This model underestimates the damping rate, because it is based on an inviscid solution. Another limitation of this analysis is that it is derived for small oscillations; however, it provides easy theoretical based equations for the study of the oscillation phenomena.

In 1968, Miller and Scriven[39] extended the analysis of oscillation in viscous media in a more rigorous way by solving the NS equations assuming that the fluids are isothermal, incompressible and Newtonian and the fact that gravitational forces are negligible

$$\frac{\partial \vec{\mathbf{v}}}{\partial t} = -\frac{1}{\rho}\nabla p + v\nabla^2 \vec{\mathbf{v}} \quad (8)$$

where p is the pressure, ρ is the density, v the specific viscosity and **v** the velocity. The solution of the NS equation uses spherical harmonics for approximating the velocity and vorticity terms. The solution informs about the decay factor and the angular frequency of oscillation. For the sake of the length of the paper, we are not going to present the solution procedure by Miller and Scriven, nor all the cases whether the fluids are liquids or gases. On the other hand, we will discuss on the results for gas bubbles in a liquid. The solution to the NS equations can be obtained analytically only for the two asymptotic approximations, either for a low viscosity fluid or a high viscosity one. The low viscosity case agrees with lamb's studies,[4] since NS equation is simplified to Laplace equation. For the high viscosity case, a point is reached which oscillations no longer occur and the deformed bubble returns slowly to the spherical shape aperiodically. The frequency of oscillation and the decay factor are given by equations (9) in Table 1, while for other cases numerical solution of the NS is needed.

A few years later, Prosperetti[11,12,46] found that even though previous work based on a normal mode approach was useful for forced oscillations, free oscillations about the spherical shape could not be represented in terms of a single value of the frequency ω and the damping parameter b, but in terms of modulated oscillations (equation (10)). The solution proposed was based on the linearisation of the equations of motion subject to the boundary conditions and the irrotational approximation which enabled them to obtain analytical solutions for the asymptotic limits, for small times and large times

$$A_n(t) \propto \exp[-b(t) \pm i\varpi(t)]t \tag{10}$$

The asymptotic values for ω and b for $t \to \infty$ are those given by the normal mode analysis and for $t \to 0$ are only available for the two cases in which only one fluid has significant dynamical effects, such as free drop in air or a gas bubble. The calculus of ω and b turns out to be a hard problem. In between the extreme cases, the model only predicts when the viscosity is small.

In parallel to the mathematical study, the oscillating regimes of gas bubbles and their shape in different regimes have been characterised on the basis of dimensionless numbers such as Weber, Reynolds, Morton and Eötvos (equation (11)), to capture the effect of the physical properties of the liquid

$$\begin{aligned} \mathrm{We} &= \frac{d_b U_B^2 \rho_L}{\sigma},\ \mathrm{Re} = \frac{\rho_L U_B d_b}{\mu}, \\ \mathrm{Mo} &= \frac{g\mu^4}{\rho\sigma^3},\ Eo = \frac{(\rho_L - \rho_G) g d_{eq}^2}{\sigma} \end{aligned} \tag{11}$$

where d_b is the bubble diameter, U_B the bubble velocity, ρ_L the liquid density, μ the liquid viscosity and σ the surface tension.[47,48] As Figs. 3 and 4 show, bubble shape changes with its size, and thus, the drag coefficient is affected.[49] As a result, the terminal velocity of the bubble not only depends on its size but also on the oscillation of the bubbles.

Modelling rising and oscillating bubbles lie within the inherently difficult free boundary problems which consists on having to prescribe boundary conditions at places where the position of the boundary is not known. Joseph[50] proposed a solution framework to free boundary problems by formulating the problem in a slightly perturbed domain and defining the change in characteristic size of the domain as the small perturbation parameter. This approach is also known as a domain perturbation technique. The solution in the perturbed domain is presumed known in some reference domain and is obtained in a power series in the perturbation parameter where the coefficients are the substantial derivatives of the variables evaluated, the velocity potential, the frequency of oscillation and the bubble shape function. Tsamopoulos and Brown[42] combined the domain perturbation technique proposed by Joseph[50] with the Poincare–Linstedt expansion method,[51] to analyse the modes of oscillation of inviscid bubbles and drops using a sphere as starting bubble shape. The problem related to the viscous boundary layer at both sides of the interphase is not tackled, since one of the phases is gas, whose hydrodynamic effects can be neglected. However, for bubbles and drops, the study makes perfect sense. Thus, the problem is formulated as the motion of a bubble assuming time periodicity, and irrotational and incompressible flow involving:

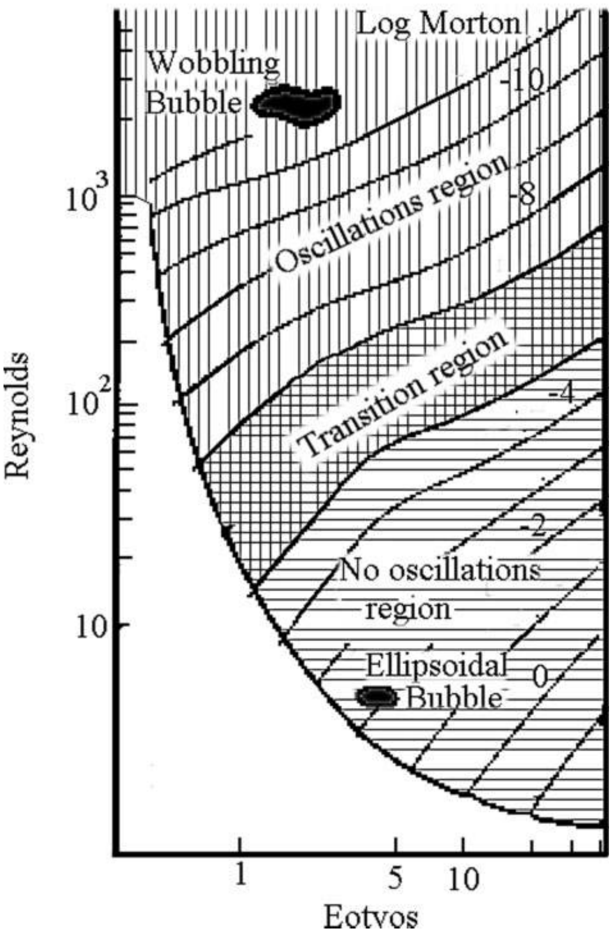

4 Oscillation regime of bubbles (based on Ref. 34)

Table 1 Oscillation decay and frequency for limiting cases

	Decay		Oscillation frequency
Low viscosity	$\frac{(2n+1)(n+2)\nu_L}{R^2}$	(9a)	Equation (1)
High viscosity	$[\text{equation (1)}]^2 \frac{(2n+1)R^2}{2(n+2)(2n^2+1)\nu_L}$	(9b)	N/A

(i) the Laplace equation
(ii) the far field boundary condition
(iii) the Bernoulli equation for the pressure
(iv) the kinematic condition that relates the shape of the surface and the velocity field
(v) the balance of dynamics and capillarity pressure across the interface
(vi) the time periodic conditions
(vii) the constant volume condition
(viii) the definitions for the amplitude
(ix) the phase of the oscillatory motion.

The variable domain is mapped so that the bubble surface is immobilised, introducing a change in the radial coordinate as given by equation (12) (see also Fig. 1)

$$r=\eta \mathrm{F}(\theta,t) \tag{12}$$

where $\mathrm{F}(\theta,t)$ is the function describing the radial coordinate of the bubble surface as a function of the angular coordinate and time and η the initial radius. In order to approximate the solution of the nonlinear partial differential equations defined in a perturbed domain, the variables are expanded using the Poincare–Linstedt method,[51] taking A, the amplitude of the oscillation, as the expansion parameter. Thus, the shape function is expanded as a series of Legendre polynomials (equations (13) and (14)) where only the term $P_n(\theta)\cos t$ contributes to the amplitude

$$\mathrm{F}(\theta,t,A)=\sum_{k=0}^{\infty}\frac{A}{k!}F^{k}(\theta,t) \tag{13}$$

with

$$\mathrm{F}^{[k]}(\theta,t)\equiv\frac{\mathrm{d}^{k}\mathrm{F}(\theta,t;0)}{\mathrm{d}A^{k}}\rightarrow\mathrm{F}^{[1]}(\theta,t)=P_n(\theta)\cos t \tag{14}$$

where P_n is the polynomial of Legendre of orden n. The expansion for velocity potential ϕ, using this approach, is of the form presented in equations (15) and (16)

$$\varphi(\eta,\theta,t;A)=\sum_{k=0}^{\infty}\frac{A^{k}}{k!}\varphi^{[k]}(\eta,\theta,t) \tag{15}$$

where

$$\varphi^{[k]}(\eta,\theta,t)\equiv\frac{\mathrm{d}^{k}\varphi(\eta,\theta,t;0)}{\mathrm{d}A^{k}} \tag{16}$$

where t is time and θ is the angular coordinate in two dimensions. Similarly, the oscillation frequency is also expanded. Montes *et al.*[24] used this method to model bubble shape and oscillation for inviscid fluids as the first stage to predict mass transfer rates. In Fig. 5, we present an example of a rising bubble in water and a picture of the bubble using high speed video techniques. The model is capable of predicting the bubble shape rather accurately.

The use of a single perturbation parameter, the oscillation amplitude, may not be enough to account for different sources of perturbation, such as those caused by the uniform motion of the bubble and those as a result of the interaction with other bubbles. Thus, Feng[43] included a second perturbation parameter in the formulation to account for these interactions or, in general, to take into account any other physical factors affecting bubble deformation. In the formulation we refer to ε_1 and ε_2 as the two perturbation parameters, with the first one to measure the effect of the uniform flow filed and the second one to scale the magnitude of the oscillatory motions that are supposed to result from other physical factors different from the flow field. The governing set of equations is similar as before, while the velocity potential Φ and the shape function of the bubble F were expanded as function of these two parameters (equations (17) and (18))

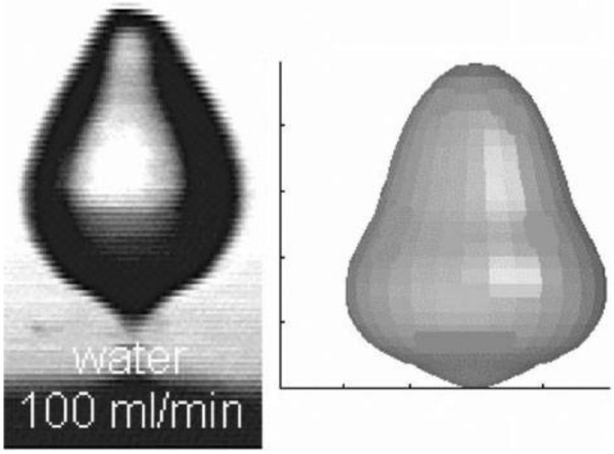

5 Comparison between modelled and recorded oscillating bubble in water[24]

$$\Phi(r,\theta,\phi,t,\varepsilon_1,\varepsilon_2)=\sum_{j=0}^{\infty}\sum_{k=0}^{\infty}\frac{\varepsilon_1^{j}\varepsilon_2^{k}}{j!k!}\Phi^{[j,k]}(\eta,\theta,\phi,t) \tag{17}$$

$$\mathrm{F}(\theta,\phi,t,\varepsilon_1,\varepsilon_2)=\sum_{j=0}^{\infty}\sum_{k=0}^{\infty}\frac{\varepsilon_1^{j}\varepsilon_2^{k}}{j!k!}\mathrm{F}^{[j,k]}(\theta,\phi,t) \tag{18}$$

where r, θ and ϕ are the spherical coordinates.

Feng[43] applied the method to model three dimensional oscillatory motion of a bubble moving in an inviscid fluid at constant velocity, but no comparison between predicted and experimental shapes was provided. Montes *et al.*[52] used this method to model bubble shape and oscillation for inviscid fluids and Fig. 6 presents an example for a bubble rising in water and the modelled shape using the multiparameter method. The model reproduces the bubbles with good agreement.

More recently, different numerical methods have been used to determine the shape of bubbles[53] which are capable of capturing the feature of bubble oscillations characteristics up to a certain point without explicitly involving the above mention variables (A,ω). One way to simulate bubbles is via the boundary integral method.[44–59] The boundary integral equation method was developed by Dr Dunn and Dr Tweed from Old Dominion University and by Dr Farassat of NASA Langley Research Center.[60,61] This method consists of formulating the problem in terms of a distribution of fundamental singularities at the boundaries, and the problem is reduced to solving integral equations by means of the Green's theorem, given by equation (19)

$$-\alpha\Phi(x_i,y_i,z_i)=\oint_{\Omega}\left(\phi\frac{\partial g}{\partial n}-g\frac{\partial\phi}{\partial n}\right)dA \tag{19}$$

where ϕ is the velocity potential and g is the green function that for a three-dimensional space is given by

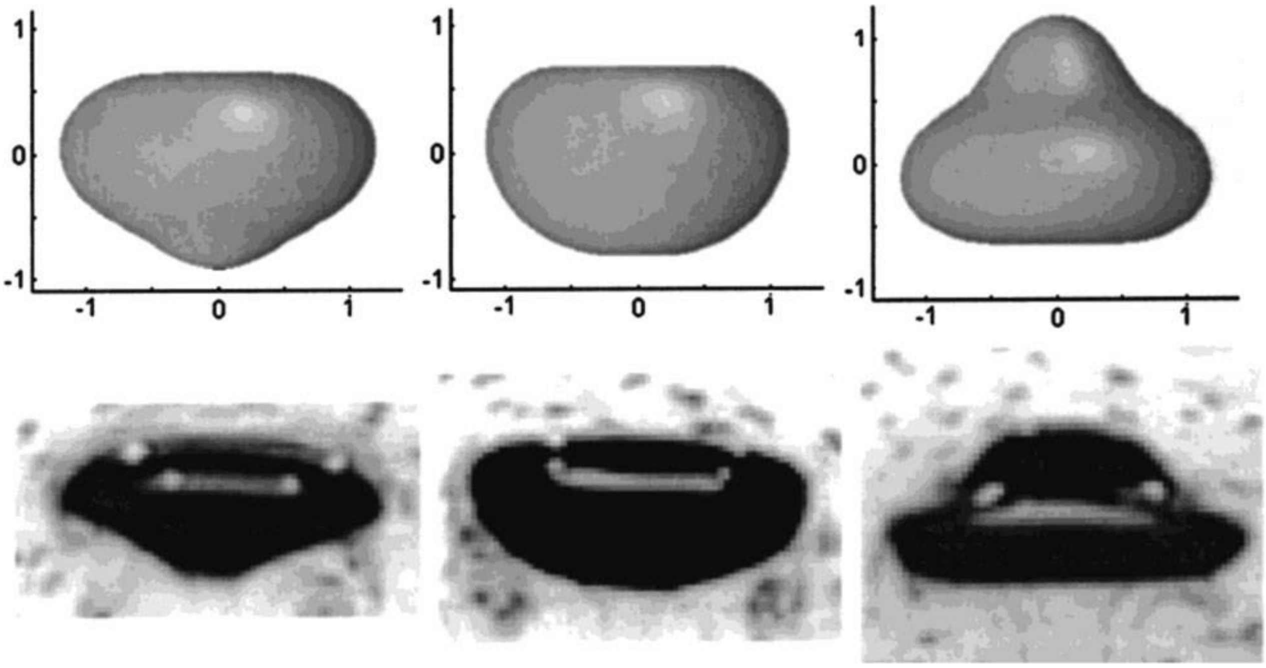

6 Axisymmetric theoretical and experimental shapes of bubbles rising and oscillating in water and with oscillation amplitude equal to 0·1 using two parameter model

equation (20)

$$g=\frac{1}{R},\ R=\left[(x-x_i)^2+(y-y_i)^2+(z-z_i)^2\right]^{1/2} \tag{20}$$

where n is the normal vector to the surface A, the area of the figure and α is 4π for all the points not belonging to the domain, while for the points of the domain, it is defined as equation (21)

$$\alpha=\lim_{R_o\to 0}\left(A_s/R_o^2\right) \tag{21}$$

Following this approach, we reduce the dimensionality of the problem by one. The velocity of the points at the boundary is obtained directly, and it is thus possible to determine the evolution of the interface in time without having to explicitly evaluate the velocity field elsewhere in the domain. It has the advantage that it does not require the discretisation of the computational domain while its main limitation is that it requires the velocity field to be expressed in terms of a potential, preventing the explicit inclusion of viscous effects. It is possible, however, to include weak viscous effects, if the vorticity is constrained to a thin region near the interface.

Different computational fluid dynamic (CFD) methods have also been used, such as front tracking,[62] as well as different solution frameworks.[63–65] Here, we briefly present the basics for some of these methods.

Front tracking methods[62] make use of markers, connected to a set of points, to track the interface, whereas a fixed or Eulerian grid is used to solve the NS equations. This method is extremely accurate but also rather complex to implement, because dynamic remeshing of the Lagrangian interface mesh is required and mapping of the Lagrangian data onto the Eulerian mesh has to be carried out. The problem becomes more complicated when multiple interfaces interact with each other, such as in coalescence and breakup processes in which case a proper subgrid model is required. Since a separate mesh is used to track the interface, there is no automatic merging of interfaces. This property is an advantage when swarm effects in dispersed flows need to be studied. The method offers considerable flexibility to assign different properties (such as the surface tension coefficient) to separate dispersed elements due to its Lagrangian basis.

Volume of fluid (VOF) techniques[66,67] use a colour function F(x,y,z,t) that indicates the fractional amount of fluid present at a certain position (x,y,z) at time t. The evolution equation for F is usually solved using advection schemes (such as geometrical advection, a pseudo-Lagrangian technique), to minimise numerical diffusion. Not only needs the value of the colour function to be determined, but also the interface orientation, which follows from the gradient of the colour function. We can point out two kinds of VOF methods depending on how the interface is represented: simple line interface calculation[66,68] and piecewise linear interface calculation.[69] Volume of fluid shows the so called artificial (or numerical) merging of interfaces which is required for modelling bubble coalescence which is limited by the size of the grid. Thus, if our system is dominated by coalescence, the VOF methods do not require specific algorithms for the merging (or breakage) of the interface such as Front tracking methods require.

The lattice Boltzmann method is due to Hardy *et al.*[70] and Broadwell.[71] This method originated from lattice gas automata, a discrete particle kinetics utilising a discrete lattice and discrete time. The lattice Boltzmann method can also be viewed as a special finite difference scheme for the kinetic equation of the discrete velocity distribution function. It has been widely used in case of a number of moving objects such as bubbles since avoids the dynamic remeshing of classical finite difference and finite element methods which becomes computationally very expensive. We can define it as a special, particle based discretisation method to solve the Boltzmann equation. However, in this method problems may arise as a result of the artificial coalescence of the bubbles.

Effect of bubble deformation and oscillation on mass transfer

So far, we have only considered the hydrodynamic part of the problem, an effort to model the bubble shape. However, there is a link between the bubble motion and the mass transfer rates, since the motion of the bubble determines the concentration profiles surrounding it and thus, the Sherwood number.

Most of the theoretical models to predict mass transfer rates from rising drops or bubbles consider their shape as a sphere. With this simplification, it is possible to solve the continuity equation including species diffusion analytically as in Ref. 72 (see equation (22) for the liquid film resistance obtained by this approach, in Table 2). Spherical shape has also been assumed to determine mass transfer rates by others for inviscid fluids,[73–75] non-Newtonian fluids[76–81] (see equation (23) in Table 2) including the effect of particle viscosity,[82,83] for slurries,[84] for oscillating flows[28,85] and for different flow regimes defined by their Reynolds number, low,[76,77,86,87] intermediate[88–93] and high Reynolds numbers[94–96] respectively. Owing to the number of parameters involved in the measurement of the mass transfer rates and the experimental error involved in measuring,[23,31] the predictions have been reasonable while providing theoretical basis.

However, as we have presented in Figs. 2 and 3, bubble shapes in gas–liquid contactors are far from spherical. Some authors have approximated them by either using regular shapes like an ellipsoid,[97–99] a spheroid[96,100] and a spherical cap[101] or considering the bubble, as if it consisted of two spherical caps.[96,97] By means of these simplifications, it was also possible to solve the continuity equation analytically to calculate the concentration profile around the bubble determining the mass transfer rates. Table 2 shows the Sherwood number for some representative bubble shapes. As a result, the authors claimed better agreement of the models with the experimental results. It is clear that these bubble shapes are closer to the real ones. Even though, researches acknowledge that the differences between the assumed shapes of the bubbles and the actual ones are behind the mismatch between the predicted and the experimental results. However, the effort of solving for different bubble shapes provides a useful insight to the effect of the bubble shape and, eventually, the effect of the modification of the bubble shape on the Sherwood number leading to the effect of bubble oscillations on it.

Together with the theoretical effort, Calderbank in 1958[102] used dimensional analysis to develop several correlations for the Sherwood number as function of the Schmidt number ($\mathrm{Sc}=\mu/\rho D_{\mathrm{AB}}$) and the Grashof number ($\mathrm{Gr}=d_{\mathrm{b}}^3\rho\Delta\rho g/(\mu D_{\mathrm{AB}})$, where μ is the liquid viscosity, ρ the liquid density, d_{b} the bubble diameter, g gravity, D_{AB} the diffusion coefficient and $\Delta\rho$ the difference in densities between the gas and the liquid phase). In this work, two regimes are differentiated, one for large bubbles, >2·5 mm, whose Sherwood number can be predicted using equation (28)

$$\mathrm{Sh}=0{\cdot}42(\mathrm{Sc})^{0{\cdot}5}(\mathrm{Gr})^{0{\cdot}33} \tag{28}$$

And the other for small bubbles, <2·5 mm, in which case, the Sherwood number is given by equation (29)

$$\mathrm{Sh}=2{\cdot}0+0{\cdot}31(\mathrm{ScGr})^{0{\cdot}33} \tag{29}$$

In between those values, the liquid film resistance increases linearly with the bubble size. These correlations can be regarded as the first result that considers the effect of bubble deformation on the volumetric mass transfer coefficient by assuming that large and small bubbles behave differently. Actually, the critical diameter limiting both classes, deformable and rigid, may not be 2·5 mm as Calderbank proposed.[102] The idea of a critical diameter for a bubble was theoretically presented by Barabash *et al.*[103] who defined the critical diameter of a stable bubble in a fluid based on a balance of forces as equation (30) in accordance with the surface stability theory

$$\frac{2\sigma}{d_{\mathrm{cr}}}=\frac{\rho_{\mathrm{L}}U_{\mathrm{B}}^2}{2} \tag{30}$$

Table 2 Sherwood and liquid film resistance k_L for representative bubble shapes*

Shape			Ref.
Spherical (Newtonian)	$k_L=2\left(\frac{D_{AB}}{\pi t}\right)^{1/2}$	(22)	72
Spherical (non-Newtonian)	$k_L=2\left(\frac{D_{AB}}{t}\right)^{1/2}\left(\frac{\varepsilon}{K/\rho}\right)^{1/2(1+n)}$	(23)	77, 112
Oblate spheroid	$\frac{\mathrm{Sh_{os}}}{\mathrm{Sh_{sphere}}}=\left[\frac{2}{3}(1+k)\right]^{1/2}\frac{2E^{1/3}(E^2-1)^{1/2}}{E(E^2-1)^{1/2}+\ln[E+(E^2-1)^{1/2}]}$	(24)	96
Prolate spheroid	$\frac{\mathrm{Sh_{os}}}{\mathrm{Sh_{sphere}}}=\left[\frac{2}{3}(1+k)\right]^{1/2}\frac{2E^{1/3}(E^2-1)^{1/2}}{E(E^2-1)^{1/2}+\sin^{-1}(1-E^2)^{1/2}}$	(25)	96
Spherical cap	$\mathrm{Sh_{sc}}=1.79\frac{(3E^2+4)^{2/3}}{E^2+4}\mathrm{Pe}^{1/2},\ \mathrm{Pe}=\frac{U_{\mathrm{B}}d_{\mathrm{b}}}{D_{\mathrm{AB}}}$	(26)	96
Ellipsoidal	$\mathrm{Sh}=0.564\left(\mathrm{Pe}\int_0^{\pi}\frac{1+2Z^3(\theta)\sin^3\theta\mathrm{d}\theta}{Z^3(\theta)}\right)^{1/2}$ $Z(\theta)=1-\left(\frac{3}{64}\right)\mathrm{We}^2[1+3\cos(2\theta)]$	(27)	101

*k_L: liquid film resistance; D_{AB}: diffusivity; t: bubble contact time; K, n: power law coefficients; ε: specific energy; E: aspect ratio of the bubble; Pe: Peclet number; We: Weber number.

where U_B is either the rising velocity of the bubbles when the dispersed elements are affected by gravitation, or the velocity of pulsations of the order of magnitude of the dispersed element, defined according to Kolmogorov's 'two-thirds' law, ρ_L is the liquid density, σ the surface tension and d_{cr} the critical diameter. In a gas–liquid system, d_{cr} is 1·5 mm so that bigger bubbles oscillate, according to Barabash *et al.*[103] Since it is common that the bubble mean diameter in process equipment is between 4 and 5 mm,[23] bubbles are always deformable.

As we can see in Figs. 2 and 3, bubbles deform as they rise[48,59] and their shape is not constant. In order to provide a theoretical basis for the effect of bubble deformation in time on the mass transfer rates, Angelo *et al.*[104] proposed in 1964 the superficial stretching theory. They suggests that the mass transfer coefficient can be characterised as a function of the stretching of the bubbles' surface and their oscillatory movement with respect to a reference state[98,105]

$$k_L a = \frac{(A_r/A_{ref})(D_{AB}/\pi t)^{1/2}}{\left[\int_0^{t/t_r} (A_r/A_{ref})^2 dt\right]^{1/2}} \tag{31}$$

where $k_L a$ is the volumetric mass transfer coefficient (a is the contact area per unit of volume and k_L is the liquid film resistance), D_{AB} is the diffusivity, t is time, A_{ref} is the area of the bubble in stable shape and A_r is the actual bubble area. Since bubble oscillation is a periodic phenomenon, a time average is required to determine the mean Sherwood number.

At this point, the aim is to develop a theoretical equation for the Sherwood number that includes the contribution of bubble deformation. When a bubble moves through a liquid, it exchanges gas from the bubble to the liquid phase. It is possible to assume that the oxygen concentration is constant at the water/air interface, but the position of the interface is not known. The oscillating movement of the bubble generates convective motions that greatly enhance the overall mass transfer rate defined by the derivative of concentration with respect to the normal to the bubble surface. The main assumption in the formulation of the mass transfer problem is that the momentum and mass transfer equations are only coupled through the velocity field.[42,43] Thus, the computation of theoretical velocity profiles surrounding an oscillating bubble is the first and crucial step in the development of accurate mass transfer correlations[50] so that the velocity profile, as a result of the oscillations, will be responsible for the mass transfer rates.

Following Tsamopoulos and Brown's work,[42] the momentum transfer problem can be solved first and the resulting velocity field is used to formulate the mass transfer problem in equation (32). The solution to the hydrodynamic problem was obtained assuming that oscillations occur inside an inviscid fluid.[42] On the other hand, mass transfer rates from oscillating bubbles are affected by the mode and amplitude of the oscillations. Since the velocity field is described by a velocity potential, the equations are linear and it is possible to solve them separately for each mode of oscillation. Thus, the mass transfer problem is thus formulated independently for each of the oscillating modes and the contribution of each mode of oscillation can be combined to represent the overall mass transfer rates using a weighted contribution for each mode. The contribution of each mode of oscillation to the overall mass transfer problem, however, it cannot be evaluated experimentally, because it is not possible to determine local mass transfer rates. Based on these assumptions,[42,43,106] Montes *et al.*[24] developed a theoretical equation for the Sherwood number of bubbles in the oscillatory regime given by equation (32)

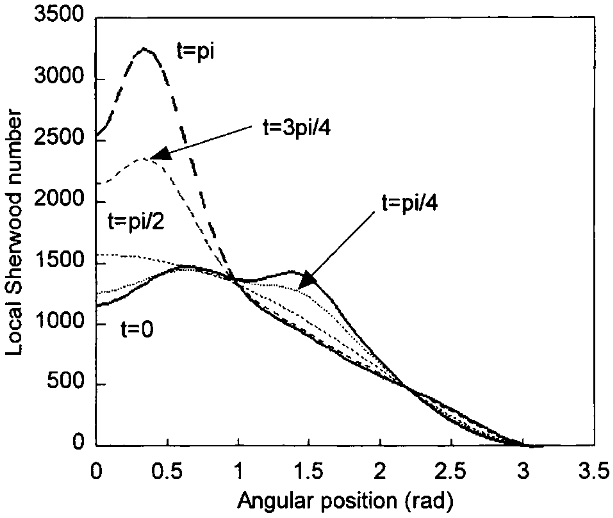

7 Local Sherwood number as function of angular position: d_b=4 mm, A_o=0·4, n=2 (Ref. 24)

$$\mathrm{Sh} = \frac{2}{\pi^{1/2}}\mathrm{Pe}^{1/2}\left(I_{n1} + I_{n2}\frac{A}{\omega_n^2}\mathrm{We}^{1/2}\right) \tag{32}$$

where

$$I_{n1} = \frac{3}{4\pi 2^{1/2}}\int_0^{\pi}\int_0^{\pi} N(\theta)\frac{\partial r}{\partial v}\left[F_n^2 + \left(\frac{\partial F_n}{\partial \theta}\right)^2\right]^{1/2} \sin\theta \mathrm{d}\theta \mathrm{d}t \tag{33}$$

$$I_{n2} = \frac{3}{8\pi}\int_0^{\pi}\int_0^{\pi} N(\theta)\frac{\partial r}{\partial v}\left[F_n^2 + \left(\frac{\partial F_n}{\partial \theta}\right)^2\right]^{1/2} \sin\theta \mathrm{d}\theta \mathrm{d}t \tag{34}$$

$$N(\theta) = \frac{\sin^2(\theta)}{(1 - 3\cos\theta/2 + \cos^3\theta/2)^{1/2}} \tag{35}$$

where We is the Weber number, Pe the Peclet number, both defined above, F the shape function, θ the angular coordinate and t time. In Fig. 7, we present the local Sherwood number at different positions along the bubble surface resulting from an oscillating bubble for the dominant mode of oscillation n=2 for a gas bubble of 4 mm with an initial oscillation amplitude of 0·4. On the figure, we show the dimensionless time t, with respect to a period of bubble oscillation 2 pi. The maximum values for the Sherwood number are found close to the top of the bubble.

A few years later, Martín *et al.*[37] introduced the effect of liquid viscosity on the mass transfer of oscillation bubbles by coupling approximate solutions for the velocity potential at high, intermediate and low Reynolds numbers,[90,95] with Calderbank and Lochiel's work[96] where the Sherwood number was given as

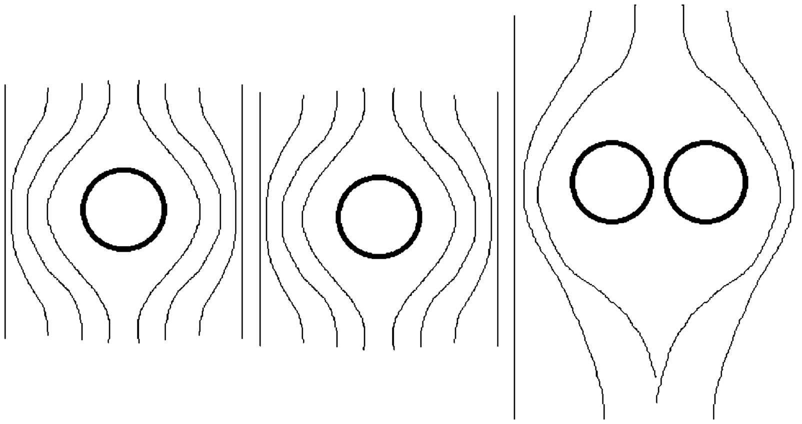

8 Effect of distance between two bubbles on flow lines surrounding them

function of the velocity profile as given by equation (36)

$$Sh = \left(\frac{2}{\pi}\right)^{1/2} Pe^{1/2} \left[\int_0^{\pi} V_{\theta}^{*}|_{r^{*}=1} \sin\theta \sin\theta d\theta \right]^{1/2} \quad (36)$$

where V_{θ} is the angular velocity at the bubble surface. The oscillation decay was included in Tsamopoulos and Brown's formulation[42] as proposed by Valentine *et al.*[38] (see equation (6)). For low viscosity fluids, the solution agrees with that provided by Montes *et al.*,[24] while for high viscosity, the oscillations are absorbed as viscous dissipation and the bubbles behave as rigid.

Recently, numerical approaches[107] and CFD simulations have also been carried out, namely Refs. 108 and 109, to calculate the velocity profile of the rising bubble and the Sherwood number. The studies for individual bubbles are accurate and are useful to develop dimensionless correlations for the Sherwood number of the bubbles. However, these simulations cannot be directly used for modelling a complete bubble column since the computational burden increases with the number of bubbles inside the gas–liquid contact equipment and makes infeasible the solution of a complete bubble column.

Bubble coalescence: contact area versus bubble oscillation.

The formation of bigger bubbles, due to coalescence (see Fig. 3), has two main effects on the hydrodynamics with an important result in the mass transfer rates. On the one hand, there is a reduction in the contact area available, which for a long time was considered as a drawback for mass transfer operations in bubble columns.[23] On the other hand, bigger bubbles are more deformable.[20] The relationship between the oscillation amplitude and the bubble size is difficult to determine since bubble oscillation amplitude depends on the liquid turbulence but increases greatly from zero as soon as the bubble oscillation behaviour changes from a rigid bubble to an oscillating bubble.[24] However, these oscillations increase the mass transfer rate due to the modification of the contact times and the concentration profiles surrounding the bubbles.[24,37] Furthermore, there is another effect of bubble coalescence on the velocity and concentration profiles. As two bubbles get closer, like those about to coalesce, there is a reduction in the concentration gradient in the vicinity of the bubble surfaces (see Fig. 8). Sherwood number drops from 2, due to molecular diffusion, to 1·98, when the distance between centres is 100 times the sphere bubble radius, to 1·6, if the former distance is four times the bubble radius, and in the case bubbles touch each other, the Sherwood number reaches a minimum value of 1·386.[73]

In the case of drops, Defrawi and Heideger[110] reported that there is an increment in the mass transfer rates immediately after coalescence, followed by a rapid fall to zero, rebound to an intermediate value and finally decay to the level expected for an undisturbed drop, with the result of a net decrease in the mass transfer rate. In the case of bubbles, the contribution of bubble coalescence to mass transfer was studied by Martín *et al.*[111] In that paper, the authors proved experimentally for different liquid fluids that although coalescence decreases mass transfer rate from bubbles, deformable bubbles can, in certain cases, balance the decrease in mass transfer rate due to the reduction in superficial area. This trade-off can then be used to avoid the harmful effect of coalescence on the mass transfer rate in the operation of bubble column reactors.

Mass transfer in bubble columns

Many research groups only focus on the hydrodynamics as we saw in the section on 'Hydrodynamics of bubble oscillations', and thus, there is a need for integrating hydrodynamic and mass transfer studies. We focus on the study of bubble columns since the bubble deformations are due to the fluid flow generated inside when injecting the gas with no other mechanical energy input such in the case of stirred tank reactors. As we have commented in the section on 'Effect of bubble deformation and oscillation on mass transfer', the volumetric mass transfer coefficient k_La is function of the contact area a, and the liquid film resistance k_L calculated through the Sherwood number. k_La actually depends on bubble shape, deformation and oscillations in both variables.[24,111] In short, on the one hand, the shape of the bubbles plays an important role in the total contact area. On the other hand, bubble deformation determines the velocity profile and concentration gradients surrounding the bubble.

For quite some time, modelling of bubble column reactors was made on the assumption that the bubbles were spherical.[112] The first model available in the literature combines the liquid film resistance, which is

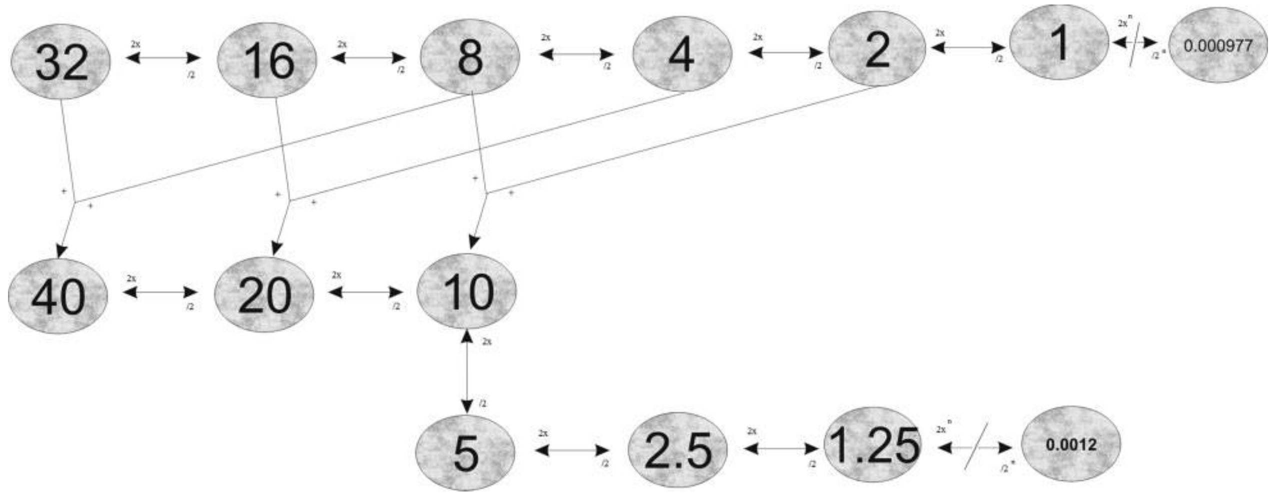

9 Scheme of relative size of bubbles present in bubble columns reactor and coalescence and breakup processes allowed[19]

calculated through Higbie's theory[72] (equation (22)), with the specific area of the dispersion a, computed using the correlation determined in Calderbank's studies[113] (equation (37))[77,112]

$$a = 1{\cdot}44\left(\frac{\varepsilon^{0{\cdot}4}\rho^{0{\cdot}2}}{\sigma^{0{\cdot}6}}\right)\left(\frac{u_G}{U_B}\right)^{0{\cdot}5} \tag{37}$$

where ε is the energy input to the system, the product between the superficial gas velocity u_G and the gravity g, U_B the rising velocity of the bubbles, ρ the liquid density and σ the surface tension. This model can be modified to simulate non-Newtonian liquids by using equation (23) for predicting k_L as proposed by Kawase's group.[77,112]

An evolution of this model was presented by Shimizu *et al.*[114] who combined the above mentioned Higbie's theory with a population balance, based on the models proposed by Prince *et al.*[115] and Pohorecki *et al*, [116] to determine the gas–liquid contact area. This model also assumes that the bubbles are spherical for determining k_L and a. The subsequent evolution of this idea was the use of CFD simulation to calculate the hydrodynamics of the bubble column.[117] This approach allowed the calculus of the energy dissipation across the tank (ε in equation (37)), responsible for the breakup and coalescence processes across the tank, which is used in a population balance to compute the bubble size distribution. Higbie's theory is used again to determine the k_L. CFD simulations still consider spherical particles[118–121] mainly due to the computational burden related to the use of a different geometry. Another limitation of the CFD codes in terms of prediction is the large number of adjustable parameters involved in the breakup and coalescence closures, which helps simulate the experimental results but makes really complex the prediction of non validated gas–liquid systems. Recently,[18] a correction factor has been implemented to account for the effect of the bubble shape on Higbies' theory,[72] with good predicting capabilities over a wide range of experimental results. This result is interesting to drive the research towards the implementation of the effect of bubble oscillation into the prediction of the mass transfer rates in bubble column reactors.

So far, the contribution of the oscillation bubbles has been neglected mainly due to the computational complexity of implementing all the contributions within the same framework. In order to evaluate the effect of bubble oscillations to the mass transfer rates in bubble columns, Martín *et al.*[19,20] went a step back from the CFD so as to be able to couple the theoretical equations for the Sherwood number of that include the effect of bubble oscillation[21,92,99] with a population balance based on those proposed to compute the bubble size distribution.[114–121] The actual area of each bubble class is calculated depending on the shape of the bubble based on its size.

The implementation of the population balance needs to account for the trade-off related to coalescence presented in the section on 'Bubble coalescence: contact area versus bubble oscillation'. To include it in the prediction of the mass transfer rates, the bubble dispersion evaluated in the model needs to take into account both bubble sizes, the initial bubbles that collide and the resulting coalesced bubble. Therefore, a new scheme of the bubbles present in the dispersion was suggested which allows that the bubbles involved in breakup and coalescences processes be defined so as to evaluate whether the area lost by coalescence of two bubbles is balanced with the enhancement in the liquid film resistance, as a result of the deformability of the bigger bubble resulting from the process.[37] Figure 9 shows the bubble scheme proposed by Martín *et al.*[19] It represents the relative volumes of the bubbles that are present at the column if the initial class generated at the orifice has a volume of 8 units. Most of the common coalescence and breakup processes are allowed, such as those involving bubble coalescence between two bubbles of similar sizes and bubble breakup into identical bubbles. Thus, in Fig. 9, '2X' implies coalescence of two bubbles of the previous size resulting in a bubble of the next class. '/2' represents that a bubble of that class can be obtained by bisection of a bubble of the previous size and '+' indicates that those bubble classes are allowed to coalesce.

In order to model bubble coalescence we analyze the collisions between bubbles. Prince and Blanch[115] proposed a model for bubble coalescence in bubble columns where the coalescence for two bubbles, i and j, is given by the product between the collision frequency and the efficiency by which those collisions derive in coalescence

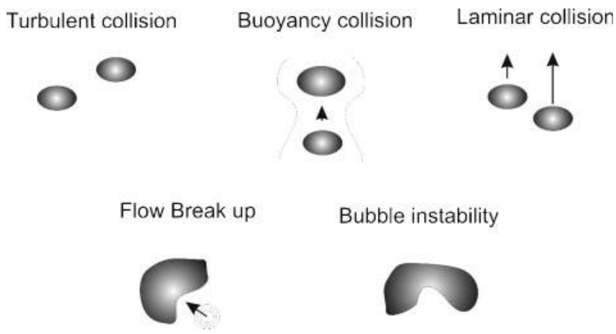

10 Breakup and coalescence mechanisms in bubble column

(equation (38))

$$C_{ij} = \left(\sum_{m} \theta_{ij}^{m}\right)\lambda \tag{38}$$

The total collision frequency C_{ij} is reported to be the sum of different mechanisms θ_{ij}^{m}, such as turbulent, buoyancy and laminar stress collisions[115,116] and the collision efficiency λ.

Among the collision mechanisms in Fig. 10, turbulence collision rate θ_{ij}^{T} corresponds to the collision frequency between two bubbles in turbulent regime due to the relative motion of the bubbles. It is based on the collision theory for ideal gases. Buoyancy collision rate θ_{ij}^{B} occurs when a bubble reaches another bubble. The wake of the previous bubble speeds up the second one into collision. Finally, the laminar stress collision rate θ_{ij}^{LS} occurs when a bubble overtakes another bubble. Table 3 presents the equations for the different mechanisms where n_i is the concentration of bubbles of class i, S_{ij} the collision cross sectional area, between bubbles is defined as equation (39), and u_t the turbulent velocity for bubbles of diameter d_b in the inertial subrange of isotropic turbulence (equation (40)), u_{ri} the rising velocity (equation (42)), σ the surface tension, ρ_L the liquid density and d_{bi} the diameter of the bubble of size i. Laminar stress collision rate, occurs when a bubble overtakes another bubble, where U_l is the liquid velocity, r_c the radial coordinate, D_c is the bubble column diameter and u_G the superficial gas velocity.

Coalescence probability depends on the intrinsic contact between bubbles. After bubble collision, a drainage channel is developed and the liquid film between the bubbles is partially or totally drained. Coulaloglou and Tavlarides[122] defined the collision efficiency λ between bubbles as a probability function which depends on the relationship between the time required for film drainage and the contact time of the bubbles. The coalescence is thus controlled by the drainage of the liquid film between two bubbles and the effect of the physical properties of the liquid plays an important role. Marucci[123] proposed a model for the drainage of the liquid film based on drainage velocity which was the origin for later studies by Ghosh and Chesters[124,125] who developed models for determining the efficiency of bubble collisions depending on the dominant regime, the presence of surfactants on the bubble surface, the effect of liquid viscosity, etc. These models are really useful in an attempt to avoid adjustable parameters for predicting the effect of the physical properties of liquid phase on the coalescence rates.[20,126] Table 4 shows the equations for computing the coalescence efficiency, where τ_{ij}, is the contact time of two bubbles i and j, t_{ij}, their drainage time, and h the film thickness either initial or final for low viscous fluids. In case of viscous ones or in case of the presence of surfactants eq. (48) will be modified and we refer to the literature[20,124,125] for different models.

The energy dissipated in the flow deforms and eventually breaks the bubbles. Different bubble breakage rates are proposed in the literature to model the bubble size distribution (see Fig. 9). For bubble breakup due to the effect of turbulent eddies, Prince and Blanch[115] modelled bubble breakage of a bubble i assuming that the bubble collides with turbulent eddies, as equation (50)

$$B_i = \left(\theta_{i,eddy}^{T}\right)\kappa \tag{50}$$

Therefore, the breakup rate is written as the product between the turbulent collision rate of bubbles and turbulent eddies $\theta_{i,eddy}^{T}$ and the efficiency of those collisions κ. The collision rate is given as that between two bubbles[115,116]

$$\theta_{ie} = n_i n_e S_{ie}\left(u_{ti}{}^2 + u_{te}^2\right)^{0\cdot5} \tag{51}$$

The turbulent velocity of the eddies can be written as equation (52)[115,116]

$$u_{te} = 1\cdot4\varepsilon^{1/3} d_e^{1/3} \tag{52}$$

The efficiency of the breakage is calculated as the ratio between the critical energy to break a bubble and the one available as equation (53)[115,116]

$$\kappa_i = \exp\left(-\frac{u_{ci}^2}{u_{te}{}^2}\right) \tag{53}$$

where the critical vortex velocity capable of breaking a bubble of diameter d_{bi},[115] is given as equation (54) follows and u_{te} as before

$$u_{ci} = \left(\frac{We_c \sigma}{d_{bi}\rho_L}\right)^{0\cdot5} \tag{54}$$

The key parameter here is the critical Weber number.[115,116] Martín *et al.*[19,20,126] used it as an adjustable parameter and related it to the physical

Table 3 Basic model for collision frequency in bubble column[115,19]

Collision mechanism		Contact area		Collision velocity	
$\theta_{ij}^{T} = n_i n_j S_{ij}(u_{ti}^2 + u_{tj}^2)^{0.5}$	(39)	$S_{ij} = \frac{\pi}{16}(d_{bi} + d_{bj})^2$	(40)	$u_t = 1.4\varepsilon^{1/2} d_b^{1/3}$	(41)
$\theta_{ij}^{B} = n_i n_j S_{ij}(u_{ri} - u_{rj})$	(42)			$u_{ri} = \left(2.14\frac{\sigma}{\rho_L d_{bi}} + 0.505 g d_{bi}\right)^{0.5}$	(43)
$\theta_{ij}^{LS} = n_i n_j \frac{4}{3}\left(\frac{d_{bi}}{2} + \frac{d_{bj}}{2}\right)^3\left(\frac{dU_1}{dr}\right)$	(44)			$\frac{dU_1}{dr_C} \approx \frac{U_1}{D_C/2} = \frac{0.787(gD_C u_G)^{1/3}}{D_C/2}$	(45)

properties of the liquid phase with good results in predicting the bubble mean size for water and viscous liquids.

There are other models for bubble breakup. Here, we only mention three more:

(i) Luo and Svendsen[127] proposed another model for the breakup frequency which accounts for the total gas phase in the bubble column reactor (equation (55)). This is one of the most common breakup closures implemented in CFD packages.

$$B_{\mathrm{i}}=0.923(1-\varepsilon_{\mathrm{g}})\left(\frac{\varepsilon}{d_b}\right)^{1/3}$$

$$\frac{(1+d_e/d_b)^2}{d_b^2(d_e/d_b)^{11/3}}e^{\left[-\frac{\pi\sigma d_{\mathrm{b}}^2 j\left[f_v{}^{2/3}+(1-f_v)^{2/3}-1\right]}{(\pi\rho_{\mathrm{L}}\beta/12)(\mathrm{d_e/d_b})^{11/3}(d_{\mathrm{b}}\varepsilon)^{2/3}}\right]} \tag{55}$$

where d_{e} is the diameter of the eddies, d_{b} the bubble diameter, ε_{g} the gas hold-up, f_{v} the fraction in which a bubble is broken down, ε the turbulent energy in the column and β a coefficient of the model.

(ii) Martinez-Bazán *et al.*[128,129] developed another model for bubble breakup efficiency based on the stability of a jet (equation (56)). The forces under consideration are those which maintain bubble size, surface tension, and those which attempt to deform it, the turbulent energy. The model proposed considers that the highest probability for a bubble is to break into two equal daughter bubbles and relies on a couple of parameters that are calculated for the specific working system.[24,30,128,129]

$$B_{\mathrm{i}}=n_{\mathrm{i}}0\cdot25\frac{\left[8\cdot2(\varepsilon d_{\mathrm{b,i}})^{2/3}-(12\sigma/\rho_{\mathrm{L}}d_{\mathrm{b,i}})\right]^{1/2}}{d_{\mathrm{b,i}}} \tag{56}$$

(iii) Alternatively, bubbles can also break due to instability as presented by Wang and Wang.[119]

As presented in Fig. 3, bubble oscillations are caused because of the bubble interactions. For example, when two bubbles collide they get deformed and oscillate towards a stable shape in accordance with its size. Also after coalescence when the new bubble has an initial shape, according to the individual bubbles which generated it and it oscillates to an equilibrium shape, or after breakup, because the elongation previous to bubble breakage deforms the bubble and the two bubbles resulting for the process oscillate to reach a stable shape according to their new size after.[34,39] In order to compute the oscillation amplitude of the bubbles in the swam and to calculate the surface area provided by each bubble, Kulkarni *et al.*[130] proposed a useful correlation that determines the aspect ratio of the bubble E, as function of the Eötvos dimensionless number (equation (57)). The amplitude of oscillation can be related to the deformation as expressed in equation (58)

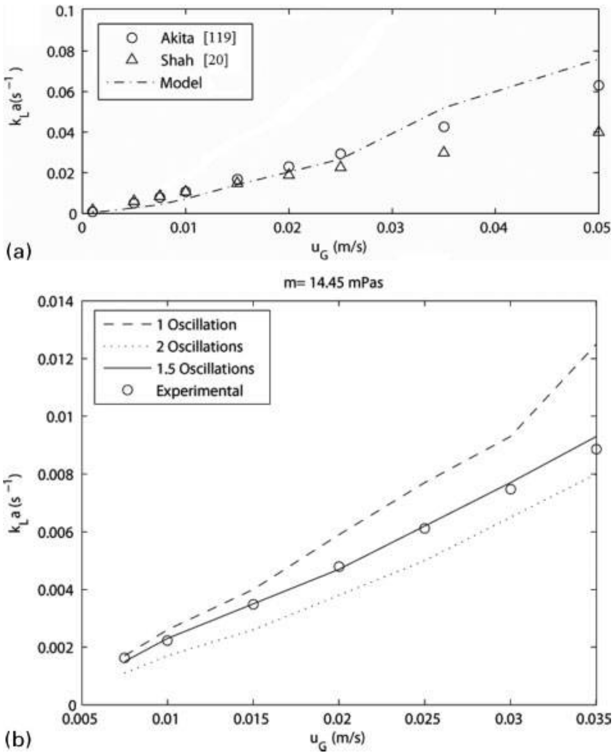

a inviscid fluids; *b* viscous fluids

11 Prediction capacity of mass transfer rates using models accounting for bubble oscillation

$$E=\frac{1}{1+0\cdot163\mathrm{Eo}^{0\cdot707}} \tag{57}$$

$$A=\frac{1-E}{2E} \tag{58}$$

Martín *et al.*[19,20] coupled a population balance with the Sherwood number for oscillating bubbles developed by Montes *et al.*[24] and Martín *et al.*[111] to predict the volumetric mass transfer coefficient including the effect of bubble oscillations. Experimental results for the volumetric mass transfer coefficient[23,131,132] and the bubble mean size[23,131] in bubble columns were used to validate the model.

For air–water systems, it was found that the prediction of the volumetric mass transfer coefficient revealed higher values than the empirical ones based on the correlations in the literature.[23,131,132] The authors realised that the presence of other bubbles may modify the velocity and concentration profiles surrounding the

Table 4 Coalescence efficiency in pure liquids

Breakup efficiency	Contact time[115]	Drainage time[115,123]
$\lambda_{\mathrm{ij}}=\exp\left(-\frac{t_{\mathrm{ij}}}{\tau_{\mathrm{ij}}}\right)$ (46)	$\tau_{\mathrm{ij}}=\frac{(0.5d_b)^{2/3}}{\varepsilon^{1/3}}$ (47)	$t_{\mathrm{ij}}=\left(\frac{(0.5d_{\mathrm{ij}})^3\rho_{\mathrm{L}}}{16\sigma}\right)^{0.5}\ln\left(\frac{h_0}{h_{\mathrm{f}}}\right)$ (48)
		$d_{\mathrm{ij}}=\left(\frac{2}{d_{\mathrm{bi}}}+\frac{2}{d_{\mathrm{bj}}}\right)^{-1}$ (49)

bubbles since the presence of bubbles does not allow a complete development of the profiles and thus the actual Sherwood number should be smaller than the one predicted by the theoretical equations.[23,111] This phenomenon had already been discussed by Lamont and Scott.[133] Thus, Martín *et al.*[19] used the corrections proposed by Lamont and Scott[133] in which case, as shown in Fig. 11*a*, it is possible to predict the mass transfer rates.

There are an increasing number of processes involving mass transfer to viscous fluids such as biochemical processes, which demands further effort to understand the effect of liquid viscosity on bubble oscillations and its effect on the mass transfer rates. Liquid viscosity decreases the mass transfer rate due to a decrease in the molecular movement on the surface of the bubble, reducing the diffusivity and the surface removal. Moreover, the velocity gradients around bubbles are also reduced since liquid viscosity attenuates bubble oscillations by absorbing the oscillation energy.[42–46] The hydrodynamics is controlled by the viscosity of the liquid, defining the breakup and coalescence rates. Bubbles in viscous fluids are more stable in the flow and, as a result, We_c increases with viscosity. A correlation between We_c and liquid viscosity was found that allowed bubble mean size prediction in bubble columns operating with viscous fluids. Furthermore, bubble collision, breakup and coalescence processes provides an initial oscillation amplitude which enhances mass transfer with respect to rigid bubbles. An important feature to point out is that bubble oscillations are only partially absorbed by viscous dissipation because the processes the bubbles experience (collisions, coalescence and breakup) provide them with an initial oscillation amplitude. The characteristic bubble oscillation time turned out to be that corresponding to 1·5 bubble oscillations[20] (see Fig. 11*b*)

Conclusions

Bubble oscillation is a complex phenomenon whose properties have been under study over the last decades. Its effects on a large number of fields from cavitation of flows, to gas liquid contact equipment have attracted an increasing number of researchers from different fields. In particular, from the chemical engineering perspective, bubble oscillations need to be understood to decrease the harmful effect on mass transfer rates. In general, there are two main contributions of the bubble oscillations to the mass transfer rates, their effect on the velocity profiles increasing the mass transfer and the effect on the contact area itself. By controlling or better understanding the bubble oscillations, it is also possible to mitigate the effect of bubble coalescence. Further studies are still required to take advantage of the phenomenon while minimising its drawbacks

Acknowledgement

The authors would like to acknowledge the funds from Ministery of innovation of Spain (research project no. CTQ2008-04727).

References

1. F. Savart: 'Memoire sur la constitution des veines liquides lancees par des orifices circulaires en mince paroi', *Ann. Chim.*, 1833, **53**, 337–386.
2. J. A. F. Plateau: 'Statique Experimentale et Theorique des liquides soumis aux seules forces meleculaires'; 1983, Ghent.
3. J. W. S. Rayleight: 'On the capillary phenomena of jets', *Proc. R. Soc. Lond.*, 1879, **29**, 71–97.
4. H. Lamb: 'Hydrodynamics', 6th edn; 1932, Dover/New York, Cambridge University Press.
5. M. Plesset: 'The dynamics of cavitation bubbles', *J. Appl. Mech.*, 1949, **16**, 277–282.
6. M. Plesset: 'On the stability of fluid flows with spherical symmetry', *J. Appl. Phys.*, 1954, **25**, 96–98.
7. A. Eller and L. A. Crum: 'Instability of motion of a pulsating bubble in a sound field', *J. Acoust. Soc. Am. Suppl.*, 1970, **47**, 762–767.
8. H. G. Flynn: 'Cavitation dynamics. I. A mathematical formulation', *J. Acoust. Soc. Am.*, 1975, **57**, 1379–1396.
9. H. G. Flynn: 'Cavitation dynamics. II. Free pulsations and models for cavitation bubbles', *J. Acoust. Soc. Am.*, 1975, **58**, 1160–1170.
10. W. Lauterborn: 'Numerical investigation of nonlinear oscillations of gas bubbles in liquids', *J. Acoust. Soc. Am.*, 1976, **59**, 283–293.
11. A. Prosperetti: 'Viscous effects on perturbed spherical flows', *Q. Appl. Math.*, 1977, **34**, 339–352.
12. A. Prosperetti: 'Free oscillations of drops and bubbles: the initial – value proble', *J. Fluid. Mech.*, 1980, **100**, 2, 333–347.
13. M. Plesset and A. Prosperetti: 'Bubble dynamics and cavitation', *Ann. Rev. Fluid Mech.*, 1977, **9**, 145–185.
14. M. S. Plesset and R. B. Chapman: 'Collapse of an initially spherical vapor cavity in the neighborhood of a solid boundary', *J. Fluid Mech.*, 1971, **47**, 283–290.
15. R. H. Cole: 'Underwater explosions'; 1948, Princeton, NJ, Princeton University Press.
16. J. Ellenberger amd R. Krishna: 'Shaken: nonstirred, bubble column reactors: enhacement of mass transfer by vibration excitement', *Chem. Eng. Sci.*, 2003, **58**, 705–710.
17. N. Kantarci, F. Borak and K. O. Ulgen: 'Bubble column reactors', *Process. Biochem.*, 2005, **40**, 2263–2283.
18. S. Nedeltchev, U. Jordan and A. Schumpe: 'Correction of the penetration theory based on mass-transfer data from bubble columns operated in the homogeneous regime under high pressure', *Chem. Eng. Sci.*, 2007, **62**, 6263–6273.
19. M. Martín, F. J. Montes and M. A. Galán: 'Mass transfer from oscillating bubbles in bubble columns', *Chem. Eng. J.*, 2009, **151**, 79–88.
20. M. Martín, F. J. Montes and M. A. Galán: 'Mass transfer rates from oscillating bubbles in bubble columns operating with viscous fluids', *Ind. Eng. Chem. Res.*, 2008, **47**, (23), 9527–9536.
21. R. P. Taleyarkhan, C. D. West, J. S. Cho, R. T. Lahey, R. Nigmatulin, Jr and R. C. Block: 'Evidence for nuclear emissions during acoustic cavitation', *Science*, 2002, **295**, 1868–1873.
22. A. Prosperetti and Y. Hao: 'Modelling of spherical gas bubble oscillations and sonolumi-nescence', *Phil. Trans. R. Soc. Lond. A*, 1999, **357A**, 203–223.
23. Y. T. Shah, B. G. Kelkar, S. P. Godbole and W. D. Deckwer: 'Design parameters estimations for bubble column reactors', *AIChE J.*, 1982, **28**, (3), 353–374.
24. F. J. Montes, M. A. Galán and R. L. Cerro: 'Mass transfer from oscillating bubbles in bioreactors', *Chem. Eng. Sci.*, 1999, **54**, 3127–3136.
25. S. Bretznajder, L. Lesniewicz and W. Pasiuk: *Bulk Acad. Pol. Sci. Ser. Sci. Chim. Geol. Geogr.*, 1959, **7**, 585.
26. S. Bretsznajder and W. Pasiuk: *Bulk Acad. Pol. Sci. Ser. Sci. Chim. Geol. Geogr.*, 1959, **7**, 591.
27. S. Bretsznajder, M. Jaszczak and W. Pasiuk: *Int. Chem. Eng.*, 1963, **3**, 496.
28. H. M. Blackburn: 'Mass and momentum transport from a sphere in steady and oscillatory flows', *Phys. Fluids*, 2002, **14**, (11), 3997–4011.
29. Y. G. Waghmare, R. G. Rice and F. C. Knopf: 'Mass transfer in a viscous bubble column with forced oscillations', *Ind. Eng. Chem. Res.*, 2008, **47**, (15), 5386–5394.
30. K. L. Harbaum and G. Houghton: 'Effects of sonic vibrations on the rate of absorption of carbon dioxide in gas bubble-beds', *Appl. Chem.*, 1962, **12**, 234–240.
31. K. Van't Riet: 'Review of measuring methods and results in non viscous gas liquid mass transfer in stirred vessels', *Ind. Eng. Chem. Process. Dev.*, 1979, **18**, 357–364.
32. K. Terasaka, J. Oka and H. Tsuge: 'Ammonia absorption from a bubble expanding at a submerged orifice into water', *Chem. Eng. Sci.*, 2002, **57**, (18), 3757–3765.

33. M. Martín, F. J. Montes and M. A. Galán: 'Oxygen transfer from growing bubbles: effect of the physical properties of the liquid', *Chem. Eng. J.*, 2007, **128**, 21–32.
34. J. R. Grace: 'Shapes and velocities of bubbles rising in infinite liquids', *Trans. IChemE.*, 1973, **51**, 116–120.
35. R. M. Edge and C. D. Grant: 'The terminal velocity and frequency of oscillation of drops in pure systems', *Chem. Eng. Sci.*, 1971, **26**, 1001–1012.
36. M. Martín, F. J. Montes and M. A. Galán: 'On the influence of impeller type on the bubble break-up process in stirred tanks', *Ind. Eng. Chem. Res.*, 2008, **47**, 6251–6263.
37. M. Martín, F. J. Montes and M. A. Galán: 'Approximate theoretical solutions for the Sherwood number of oscillating bubbles at different Reynolds numbers', *Chem. Eng Process.*, 2010, **49**, 245–254.
38. R. S. Valentine, N. F. Sather and W. J. Heideger: 'The motion of drops in viscous media', *Chem. Eng. Sci.*, 1965, **20**, 719–728.
39. C. A. Miller and L. E. Scriven: 'The oscillations of a fluid droplet immersed in another fluid', *J. Fluid. Mech.*, 1968, **32**, (3), 417–435.
40. R. R. Schroeder and R. C. Kintner: 'Oscillations of drops falling in a liquid field', *AIChE J.*, 1965, **11**, (1), 5–8.
41. M. Favelukis and C. Hung Ly: 'Unsteady mass transfer around spheroidal drops in potential flow', *Chem. Eng. Sci.*, 2005, **60**, 7011–7021.
42. J. A. Tsamopoulos and R. A. Brown: 'Nonlinear oscillations of inviscid drops and bubbles', *J. Fluid Mech.*, 1983, **127**, 519–537.
43. J. Q. Feng: 'The oscillations of a bubble moving in a inviscid fluid', *SIAM J. Appl. Math.*, 1992, **52**, (1), 1–14.
44. A. Prosperetti: 'Free oscillations of drops and bubbles: the initial – value problem', *J. Fluid Mech.*, 1980, **100**, (2), 333–347.
45. K. Vokurka: 'Amplitudes of free bubble oscillations in liquids', *J. Sound Vib.*, 1990, **141**, (2), 259–275.
46. A. Prosperetti: 'Viscous effects on small amplitude surface waves', *Phys. Fluids*, 1976, **19**, (2), 195–203.
47. D. Bhaga and M. E. Weber: 'Bubbles in viscous liquids: shapes, wakes and velocities', *J. Fluid Mech.*, 1981, **105**, 61–85.
48. R. C. Clift, J. R. Grace and M. E. Weber: 'Bubbles, drops and particles'; 1978, New York, Academic Press.
49. J. de Vries, S. Luther and D. Lohse: 'Induced bubble shape oscillations and their impact on the rise velocity', *Eur. Phys. J. B*, 2002, **29B**, 503–509.
50. D. D. Joseph: 'Domain perturbations: the higher order theory of infinitesimal water waves', *Arch. Ration. Mech. Anal.*, 1973, **51**, 295–303.
51. A. H. Mayfeh and D. T. Mook: 'Nonlinear oscillations'; 1979, New York, Wiley-Interscience.
52. F. J. Montes, M. A. Galán and R. L. Cerro: 'Comparison of theoretical and experimental characteristics of oscillating bubbles', *Ind. Eng. Chem. Res.*, 2002, **41**, (25), 6235–6245.
53. P. C. Chan, K. K. Kan and J. M. Stuhmiller: 'A computational study of bubble–structure interaction', *J. Fluids Eng.*, 2000, **122**, 783–790.
54. N. K. McDougald and L. G. Leal: 'Numerical study of the oscillations of a non-spherical bubble in an inviscid, incompressible liquid. Part I: free oscillations from non-equilibrium initial conditions', *Int. J. Multiph. Flow*, 1999, **25**, 887–919.
55. N. K. McDougald and L. G. Leal: 'Numerical study of the oscillations of a non-spherical bubble in an inviscid, incompressible liquid. Part II: the response to an impulsive decrease in pressure', *Int. J. Multiph. Flow*, 1999, **25**, 921–941.
56. Q. X. Wang: 'The evolution of a gas bubble near an inclined wall', *Theor. Comput. Fluid Dyn.*, 1998, **12**, 29–51.
57. Q. X. Wang, K. S. Yeo, B. C. Khoo and K. Y. Lam: 'Strong interaction between a buoyancy bubble and a free surface', *Theor. Comput. Fluid Dyn.*, 1996, **8**, 73–88.
58. Q. X. Wang, K. S. Yeo, B. C. Khoo and K. Y. Lam: 'Nonlinear interaction between gas bubble and free surface', *Comput. Fluids*, 1996, **25**, (7), 607–628.
59. E. Klaseboer and B. C. Khoo: 'Boundary integral equations as applied to an oscillating bubble near a fluid–fluid interface', *Comput. Mech.*, 2004, **33**, 129–138.
60. M. H. Dunn, J. Tweed and F. Fassad: 'The application of a boundary integral equation method to the prediction of ducted fan engine noise', *J. Sound Vib.*, 1999, **227**, (5), 1019–1048.
61. M. H. Dunn, J. Tweed and F. Fassad: 'The prediction of ducted fan engine noise via a boundary integral equation method', Proc. 2nd AIAA/CEAS Aeroacoustical Conf., State College, PA, USA, May 1996, AIAA, Paper 96-1770.
62. M. van Sint Annaland, W. Dijkhuizen, N. G. Deen and J. A. M. Kuipers: 'Numerical simulation of behavior of gas bubbles using a 3-d front-tracking method', *AIChE J.*, 2006, **52**, (1), 99–110.
63. Y. M. Lau, I. Roghair, N. G. Deen, M. van Sint Annaland and J. A. M. Kuipers: 'Numerical investigation of the drag closure for bubbles in bubble swarms', *Chem. Eng. Sci.*, 2011, **66**, 3309–3316.
64. F. Raymond and J. M. Rosant: 'A numerical and experimental study of the terminal velocity and shape of bubbles in viscous liquids', *Chem. Eng. Sci.*, 2000, **55**, 943–955.
65. B. Figueroa-Espinoza and D. Legendre: 'Mass or heat transfer from spheroidal gas bubbles rising through a stationary liquid', *Chem. Eng. Sci.*, 2010, **65**, 6296–6309.
66. M. Torrey and L. Cloutman: 'NASA-VOF2D: a computer program for incompressible flows with free surfaces', LANL technical report LA-10612-MS
67. W. F. Noh and P. Woodward: 'SLIC (simple line interface calculation)', *Lect. Notes Phys.*, 1976, **59**, 330–340.
68. C. W. Hirt and B. D. Nichols: 'Volume of fluid (VOF) method for the dynamics of free boundaries', *J. Comput. Phys.*, 1981, **39**, (1), 201–225.
69. D. L. Youngs: 'Time-dependent multi-material flow with large fluid distortion', in 'Numerical methods for fluid dynamics', (ed. K. W. Morton and M. J. Bianes), 273; 1982, New York, Academic Press.
70. J. Hardy, O. de Pazzis and Y. Pomeau: 'Molecular dynamics of a classical lattice gas: transport properties and time correlation functions', *Phys. Rev. A*, 1976, **13A**, 1949–1961.
71. J. E. Broadwell: 'Study of rarefied shear flow by the discrete velocity method', *J. Fluid Mech.*, 1964, **19**, 401–414.
72. R. Higbie: 'The rate of absorption of a pure gas into a still liquid during a short time of exposure', *Trans. Am. Inst. Chem. Eng.*, 1935, **31**, 365–389.
73. A. H. P. Skelland: 'Diffusional mass transfer'; 1974, New York, John Wiley and Sons.
74. R. B. Bird, W. E. Steward and E. N. Lightfoot: 'Fenómenos de transporte', 2nd edn; 1992, Barcelona, Reverté.
75. S. S. Sadhal, P. S. Ayyaswamy and J. N. Chung: 'Transport phenomena with drops and bubbles'; 1997, New York, Springer.
76. Y. Kawase and J. J. Ulbrecht: 'Drag and mass transfer in non Newtonian flows through multi-particle systems at low reynolds numbers', *Chem. Eng. Sci.*, 1981, **36**, 1193–1202.
77. Y. Kawase and M. Moo-Young: 'Approximate solutions for power law fluid flow past a particle at low reynolds numbers', *J. Non-Newt. Fluid Mech.*, 1986, **21**, 167–177.
78. R. M. Wellek and C.-C. Huang: 'Mass transfer from spherical gas bubbles and liquid droplets moving through power-law fluids in the laminar flow regime', *Ind. Eng. Chem. Fund.*, 1970, **9**, (3), 480–488.
79. A. B. Jarzebski and J. Malinowski: 'Transient mass and heat transfer from drops or bubbles in slow non-Newtonian flows', *Chem. Eng. Sci.*, 1986, **41**, (10), 2575–2578.
80. S. D. Dhole, R. P. Chhabra and V. Eswaran: 'Mass transfer from a spherical bubble rising in power-law fluids at intermediate Reynolds numbers', *Int. Commun. Heat Mass Transfer.*, 2007, **34**, (8), 971–978.
81. K. Ceylan, S. Herdem and T. Abbasov: 'A theoretical model for estimation of drag force in the flow of non-Newtonian fluids around spherical solid particles', *Powder Technol.*, 1999, **103**, 286–291.
82. Z. G. Feng and E. E. Michaelides: 'Heat and mass transfer coefficients of viscous spheres', *Int. J. Heat Mass Transf.*, 2001, **44**, 4445–4454.
83. A. Saboni, S. Alexandrova, A. M. Spasic and C. Gourdon: 'Effect of the viscosity ratio on mass transfer from a fluid sphere at low to very high Peclet numbers', *Chem. Eng. Sci.*, 2007, **62**, (17), 4742–4750.
84. B. Zhao, J. Wang, W.Yang and Y. Jin: 'Gas–liquid mass transfer in slurry bubble systems I. Mathematical modelling based on a single bubble mechanism', *Chem. Eng. Sci.*, 2003, **96**, 23–27.
85. E. Ruckenstein and O. Muntean: 'Mass transfer between a bubble and an oscillating liquid', *Chem. Eng. Sci.*, 1970, **25**, 1159–1166.
86. Z. G. Feng and E. E. Michaelides: 'Mass and heat transfer from fluid spheres at low Reynolds numbers', *Powder Technol.*, 2000, **112**, 63–69.
87. M. Favelukis and R. Semiat: 'Mass transfer between a slender bubble and a viscous liquid in axisymmetric extensional flow', *Chem. Eng. Sci.*, 1996, **51**, (7), 1169–1172.
88. E. Ruckenstein: 'Prediction of rates of heat or mass transfer in complex situations by interpolating between simpler limiting cases', *Chem. Eng. Sci.*, 1982, **37**, (10), 1505–1511.

89. Y. Nakano and C. Tien: 'Approximate solutions of viscous incompressible flow around fluid spheres at intermediate Reynolds numbers', *Can. J. Chem. Eng.*, 1967, **45**, 135–140.
90. W. J. Uribe-Ramirez: 'Korchinsky Fundamental theory for prediction of single-component mass transfer in liquid drops at intermediate Reynolds numbers (10<Re<250)', *Chem. Eng. Sci.*, 2000, **55**, 3305–3318.
91. R. M. Wellek and T. Gurkan: 'Mass transfer to drops moving through power law fluids in the intermediate Reynols number region', *AIChE J.*, 1976, **22**, (3), 484–490.
92. M. H. L. Baird and A. E. Hamielec: 'Forced convection transfer around sphere at intermediate Reynolds numbers', *Can. J. Chem. Eng.*, 1962, **40**, 119.
93. Y. Nakano and C. Tien: 'Viscous incompressible non-Newtonian flow around fluid sphere at intermediate Reynolds number', *AIChE J.*, 1970, **16**, (4), 569–574.
94. H. Y. Cheh and C. W. Tobias: 'Mass transfer to spherical drops or bubbles at high Reynolds number', *Ind. Eng. Chem. Fund.*, 1968, (7), 48–52.
95. G. K. Batchelor: 'An introduction to fluid dynamics', 1st edn; 1979, Cambridge, Cambridge University Press.
96. A. C. Lochiel and P. H. Calderbank: 'Mass transfer in the continuum phase around axisymmetric bodies of revolution', *Chem. Eng. Sci.*, 1964, **19**, 471–484.
97. B. Haut and T. Cartage: 'Mathematical modelling of gas–liquid mass transfer rate in bubble columns', *Chem. Eng. Sci.*, 2005, **60**, (22), 5937–5944.
98. M. Favelukis and R. R. Mudunuri: 'Unsteady mass transfer in the continuous phase around axisymmetric drops of revolution', *Chem. Eng. Sci.*, 2003, **58**, 1191–1196.
99. A. A. Kendoush: 'Heat: mass, and momentum transfer to a rising ellipsoidal bubble', *Ind. Eng. Chem. Res.*, 2007, **46**, 9232–9237.
100. Z. G. Feng and E. E. Michaelides: 'Unsteady heat and mass transfer from a spheroid', *AIChE J.*, 1997, **43**, (3), 609–614.
101. A. A. Kendoush: 'Theory of convective heat and Mass transfer to spherical cap bubbles', *AIChE J.*, 1994, **40**, (9), 1440–1448.
102. P. H. Calderbank and M. B. Moo-Young: 'The continuous phase heat and mass transfer properties of dispersions', *Chem. Eng. Sci.*, 1961, **16**, 39–54.
103. V. M. Barabash and M. A. Belevitskaya: 'Mass transfer from bubbles and drops in mechanically agitated apparatuses', *Theor. Found. Chem. Eng.*, 1999, **29**, (4), 333–342.
104. J. B. Angelo, E. N. Lightfoot and D. W. Howard: 'Generalization of the penetration theory for surface stretch: application to forming and oscillating drops', *AIChE J.*, 1966, **12**, 751.
105. J. E. Botello-Álvarez, J. L. Navarrete-Bolaños, H. Jiménez-Islas, A. Estrada-Baltazar and R. Rico-Martínez: 'Improving mass transfer coefficient prediction in bubbling columns via sphericity measurements', *Ind. Eng. Chem. Res.*, 2004, **43**, 6527–6533.
106. J. Zhu, F. Zheng, M. L. Laucks and E. J. Davis: 'Mass transfer from an oscillating microsphere', *J. Colloid Int. Sci.*, 2002, **249**, 351–358.
107. S. S: Ponoth and J. B. McLaughlin: 'Numerical simulation of mass transfer for bubbles in water', *Chem. Eng. Sci.*, 2000, **55**, 1237–1255.
108. A. Koynov, J. G. Khinast and G. Tryggvason: 'Mass transfer and chemical reactions in bubble swarms with dynamic interfaces', *AIChE, J.*, 2005, **51**, (10), 2786–2800.
109. A. A. Ganguli and E. Y. Kenig: 'A CFD-based approach to the interfacial mass transfer at free gas–liquid interfaces', *Chem. Eng. Sci.*, 2011, **66**, 3301–3308.
110. M. Defrawi and W. J. Heideger: 'Effect of drop coalescence on mass transfer rate', *Chem. Eng. Sci.*, 1978, **33**, 35–40.
111. M. Martín, F. J. Montes and M. A. Galán: 'Bubble coalescence at sieve plates: II. Effect of coalescence on mass transfer. Superficial area versus bubble oscillations', *Chem. Eng. Sci.*, 2007, **62**, 1741–1752.
112. Y. Kawase, B. Halard and M. Moo-Young: 'Theoretical prediction of volumetric mass transfer coefficients in bubble columns for Newtonian and non-Newtonian fluids', *Chem. Eng. Sci.*, 1987, **42**, (7), 1609–1617.
113. P. H. Calderbank: 'Gas adsorption from bubbles', *Chem. Eng.*, 1967, **45**, CE209.
114. K. Shimizu, S. Takada, K. Minekawa and Y. Kawase: 'Phenomenological model for bubble column reactors: prediction of gas hold-ups and volumetric mass transfer coefficients', *Chem. Eng. J.*, 2000, **78**, 21–28.
115. M. J. Prince and H. W. Blanch: 'Bubble coalescence and break-up in air sparged bubble columns', *AIChE J.*, 1990, **36**, (10), 1485–1499.
116. R. Pohorecki, W. Moniuk, P. Bielski and A. Zdrójkowski: 'Modelling of the coalescence/redispersion processes in bubble columns', *Chem. Eng. Sci.*, 2001, **56**, 6157–6164.
117. J. B. Joshi: 'Computational flow modelling and design of bubble column reactors', *Chem. Eng. Sci.*, 2001, **56**, 5893–5933.
118. P. Chen, J. Sanyal and M. P. Dudukovic: 'Numerical simulation of bubble columns flows: effect of different breakup and coalescence closures', *Chem. Eng. Sci.* 2005, **60**, 1085–1101.
119. T. Wang and J. Wang: 'Numerical simulations of gas–liquid mass transfer in bubble columns with a CFD–PBM coupled model', *Chem. Eng. Sci.*, 2007, **62**, (24), 7107–7118.
120. M. R. Bhole, J. B. Joshi and D. Ramkrishna: 'Population balance modeling for bubble columns operating in the homogeneous regime', *AIChE J.*, 2007, **53**, (3), 579–588.
121. T. Wang, J. Wang and Y. Jin: 'Population balance model for gas–liquid flows: influence of bubble coalescence and breakup models', *Ind. Eng. Chem. Res.*, 2005, **44**, 7540–7549.
122. C. A. Coulaloglou and L. L. Tavlarides: 'Description of interaction processes in agitated liquid–liquid dispersions', *Chem. Eng. Sci.*, 1977, **32**, 1289–1297.
123. G. Marrucci: 'A theory of coalescence', *Chem. Eng. Sci.*, 1969, **24**, 975–985.
124. P. Ghosh: 'Coalescence of air bubbles at air–water interface', *Trans. IChemE A*, 2004, **82A**, 849–854.
125. A. K. Chesters: 'The modelling of coalescence processes in fluid liquid dispersions', *Trans. IChemE A*, 1991, **69A**, 259–270.
126. M. Martín, F. J. Montes and M. A. Galán: 'Theoretical modelling of the effect of surface active species on the mass transfer rates in bubble column reactors', *Chem. Eng. J.*, 2009, **155**, 272–284.
127. H. Luo and H. F. Svendsen: 'Theoretical model for drop and bubble breakup in turbulent dispersions', *AIChE J.*, 1996, **42**, 1225–1233.
128. C. Martínez-Bazán, J. L. Montañéz and J. C. Lasheras: 'On the breakup of an air bubble injected into a fully developed turbulent flow. Part 1: breakup frequency', *Fluid Mech.*, 1999, **401**, 157–182.
129. C. Martínez-Bazán, J. L. Montañéz and J. C. Lasheras: 'On the breakup of an air bubble injected into a fully developed turbulent flow. Part 2: size PDF of the resulting daughter bubbles', *Fluid Mech.*, 1999, **401**, 183–207.
130. A. A. Kulkarni, J. B. Joshi, V. R. Kumar and B. D. Kulkarni: 'Simultaneous measurement of hold-up profiles and interfacial area using LDA in bubble columns: predictions by multiresolution analysis and comparison with experiments', *Chem. Eng. Sci.*, 2001, **56**, 6437.
131. K. Akita and F. Yoshida: 'Gas hold up and volumetric mass transfer coefficient in bubble columns', *Ind. Eng. Chem. Proc. Des. Dev.*, 1973, **12**, 76–80.
132. K. Akita and F. Yoshida: 'Bubble size: interfacial area and liquid phase mass transfer coefficient in bubble column', *Ind. Eng. Chem. Proc. Des. Dev.*, 1974, **13**, 84–91.
133. J. C. Lamont and D. S. Scott: 'An eddy cell model of mass transfer into surface of a turbulent liquid', *AIChE J.*, 1970, **16**, 513–519.
134. M. Martín, J. M. García, F. J. Montes and M. A. Galán: 'On the effect of sieve plate configuration on the coalescence of bubbles', *Chem. Eng. Process.*, 2008, **47**, 1799–1809.